

# A Modular Single-Phase Bidirectional EV Charger with Current Sharing Optimization

Faik Elvan

Dept. of Electrical and Electronics Engineering  
Hacettepe University  
Ankara, Turkey  
Email: faik.elvan@hacettepe.edu.tr

Mithat Kisacikoglu

Dept. of Electrical and Computer Engineering  
University of Alabama  
Tuscaloosa, AL  
Email: mkisacik@ua.edu

**Abstract**—Developing electric vehicle (EV) technologies puts EV chargers in scope for successful integration into the smart grid. The energy and power need for grid charging of EV batteries may have an adverse impact on the distribution grid depending on the architecture of the distribution system and charging control structure employed. This effect can be minimized utilizing EV battery chargers. For the wide-scale adoption of EVs, an improvement in the charging operation of the batteries will have a huge cumulative impact on the grid. Therefore, this paper presents a bidirectional modular single-phase charger with optimized current sharing for more efficient smart grid integration. The results of the implementation have been presented to verify the proposed idea in simulation and bench-top test environments.

## I. INTRODUCTION

Developing sophisticated EV-grid integration methods is an important research topic. With a growing EV market, the mass penetration of EVs into the utility grid will result in critical issues. Solutions proposed in the literature include charging/discharging control of EV batteries to decrease distribution system congestion and to improve voltage profiles [1], [2], to decrease distribution system operating costs coordinating with renewables [3], to operate within residential micro-grids [4], or even to provide emergency relief after disasters [5]. These improvements can only be realized with proper design and control of EV chargers, which have a wide variety of configurations possible [6]–[11].

Conventional battery chargers have double-stage power conversion which takes place in two separate sections in a charger. In the first stage, numerous front-end AC-DC converters, also called PFC converters, are reported, and they reached rather high efficiencies [12]–[15]. At second stage, phase-shifted full bridge (PSFB) and variants of resonant converters are widely employed. PSFBs have approximately 96% peak efficiency and can operate with wide output voltage ranges with reported power ratings of 3-6 kW [16], [17]. Resonant converters have slightly higher efficiencies, some of them over 98%, and their rated power can range from 1-6 kW [14], [18], [19].

Studies on newer charger topologies are centered around higher efficiencies, more compactness, and bidirectional power flow, all of which can be achieved by single-stage topologies. These topologies convert AC power to DC directly in single stage, provide galvanic isolation, and can eliminate bulky DC-link capacitors used in PFC converters to provide higher efficiency in a smaller form factor. Two examples for a compact and unidirectional topology are discussed in [20], [21].

Dual-active-bridge based single-stage isolated bidirectional topologies are proposed in [22], [23]. First is rated at 1.4 kW power level, achieves 89.9% peak efficiency, and presents a modulation scheme to easily control the direction and amount of power delivered [22]. The latter operates with 230 V AC grid voltage and 400 V DC output voltage. It is rated at 3.7 kW power level with 2.2 kW/lit power density with peak efficiency higher than 96% [23].

The above chargers are mostly designed to provide their peak efficiency at or near full load conditions. However, in the scope of smart grid integration of chargers, sub-optimum operation points are preferred to maintain a sustainable grid integration without causing any overloading condition in the distribution grid. This will cause charger efficiency to be lower than the peak efficiency and will draw a high energy loss factor overall. To increase efficiency for a wide load range and to provide better grid integration, a modular design methodology is proposed in this study. Modularity brings numerous advantages, such as flexibility, ease of maintenance, and increased resilience. However, it also has disadvantages such as cost, increased control complexity, and volume.

Modular structures are widely used in the industry where their advantages overwhelm the disadvantages. They are used in power supplies [24], power factor correction applications [25], and especially grid connected photovoltaic (PV) systems [26]–[28]. A modular charger application for three-phase on-board charging is proposed in [29], and another application for fast off-board charging is proposed in [30]. However, both ideas are not implemented experimentally, and their main goal is to increase charging power to decrease charging time. Light load efficiency improvement idea proposed in [25] and [26] can be applied to EV chargers as well. Such configuration can serve well for the smart chargers which have the capability to adjust charging power of the EV, according to different grid conditions during residential Level 1/Level 2 charging. With the possibility of a wide scale electrification of the vehicles in the future, any efficiency improvement in the charging process will have a drastic cumulative impact on the efficient operation of the utility grid.

Consequently, this paper presents a modular EV charger implementation with the focus on efficiency improvement at wide range using optimization techniques. Section 2 will explain system description, information on selected topology, and state the optimization problem. Section 3 will present simulation results of various operation modes of the system.

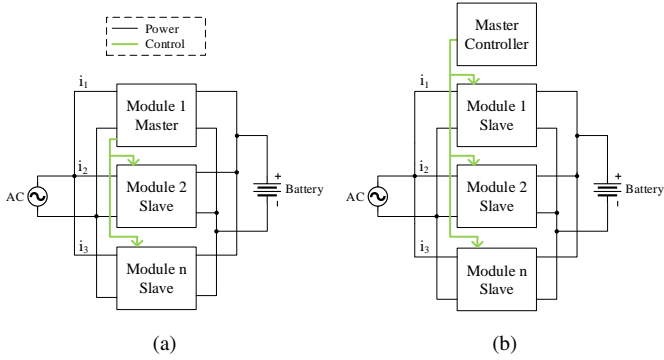


Fig. 1. Control schemes of individual modules

Section 4 will present results from the actual experimental setup. Finally, section 5 will conclude the paper and give information about planned future work.

## II. SYSTEM DESCRIPTION OF THE BIDIRECTIONAL CHARGER

### A. Modular Design Methodology

The system to be designed should provide almost constant efficiency through a wide range of load conditions. This can be achieved with a modular design approach. As reported in [26], modules can be turned on and off one by one according to the load demand. This approach can be enhanced further by a master control algorithm. Load/efficiency curves of each module can be recorded and loaded to the master controller. In a more advanced design, chargers can plot their load/efficiency curves and share this information with the master controller via a communication bus.

The master controller can orchestrate the operation of the individual modules by solving an optimization problem formed using the information on charging current and/or grid charging power information. When certain amount of charging current/grid power is demanded, master controller should select the optimal operating condition of the individual chargers based on their efficiency and set their reference commands accordingly or shut them off completely. This master controller can either be embedded inside one of the modules as shown in Fig. 1(a) or can be a separate controller with the sole task of commanding the operation of the modules as shown in Fig. 1(b). Processing power of micro controller units is increased considerably in recent years, and thus it is more suitable to follow the configuration described in Fig. 1(a) to reduce cost and design complexity. This configuration is selected in this study.

### B. Bidirectional Power Electronics Converter

For a modular EV charger unit, the topology selection is critical. The combinations of the power semiconductors, applicable topologies, and control methods are many. The design considerations for this study are selected as modularity, galvanic isolation for safety, bidirectional power flow, and compactness. Different topologies have been surveyed for modular operation [24]–[30]. For this study, the topology and the control method discussed in [22] is selected as a baseline for a modular system due to advantages such as inherent modularity, current sharing, and easily controlled bidirectional

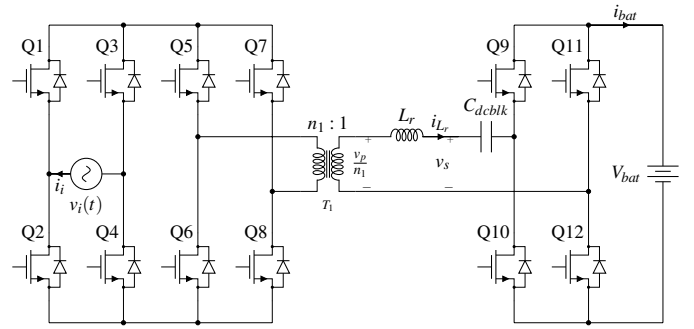


Fig. 2. Single-phase single-stage DAB AC-DC converter with a separate synchronous rectifier

power flow. Moreover, lack of electrolytic capacitors makes the design more compact, and high frequency transformer brings galvanic isolation for safety. In this study, aforementioned topology is slightly modified. Instead of bidirectional switches, a synchronous rectifier and high-frequency chopper are used. Further, power transfer is carried out by a discrete inductor instead of the leakage inductance of the transformer, and a DC blocking capacitor is added right after the inductor to compensate for any DC content in inductor current. Final configuration of the charger is given in Fig. 2.

As explained in the control algorithm proposed in [22], the charger behaves as a current sink on the input side and current source on the output side. This fact enables the chargers to be paralleled easily. Also, with the help of modular operation, optimization algorithm can be utilized to achieve efficiency increase, especially in light to middle load conditions.

As derived in [22], instantaneous DC charging current of the topology can be expressed as:

$$i_{bat}(t) = \frac{\delta V_i^2}{8 n_1^2 L f_s V_{bat}} \{1 - \cos(4\pi f_i t)\} \quad (1)$$

where  $f_s$  is the switching frequency (Hz),  $V_i$  is the input rms voltage (V),  $V_{bat}$  is the battery terminal voltage (V),  $n_1$  is the transformer turns ratio,  $L$  is the discrete inductor inductance (H),  $f_i$  is the grid frequency (Hz), and  $\delta$  is the phase-shift ratio. Assuming,  $f_s$ ,  $V_{bat}$  and  $V_i$  are constant, the only variable in the expression is  $\delta$ . This quantity can be used to control charging current, and hence, input/output power.

The output current of single-stage chargers is inherently sinusoidal with a DC offset as seen in (1). This is because the pulsating power from the AC input have to manifest itself at battery current due to single-stage AC-DC conversion. Charging with a sinusoidal-like DC current is an another research topic itself, but the studies report that charging in this manner is not harmful for Li-ion and lead-acid batteries [31], [32].

### C. Optimization Problem Statement for EV Charging

In this sub-section, we describe the optimization problem&solution to charge and discharge EV batteries using the best available charger efficiency with a modular approach. To state the optimization problem mathematically, the load-efficiency curves of individual modules should be expressed in equations with appropriate variables. Since the main two functions are to charge EV batteries and to provide power

back to the grid, the efficiency will be calculated in charging (grid-to-vehicle, G2V) and in discharging (vehicle-to-grid, V2G) modes. However, finding the optimal efficiency point depend on factors such as temperature, AC grid and battery voltages, AC and DC current rates, and switching frequency. Temperature dependency of efficiency is not taken into account in this study. Instead, the load-efficiency curves are assumed to be obtained and utilized at room temperature. Moreover, the inputs and outputs of the modules are connected in parallel, thus the voltages seen by modules from input and output sides are also the same and assumed to be constant. Furthermore, constant switching frequency operation is selected. Therefore, operating voltages and switching frequency are not included in the problem formulation.

It is assumed that grid provides positive current command for G2V and negative current command for V2G operation at a given time. Since operating voltages are assumed to be constant, grid voltage and battery voltage can be excluded from optimization problem statement, and the optimization problem in both modes of operation can be expressed with reference grid current command. Optimization algorithm will solve the optimization problem and decide the amount of current that each charger module draws or supplies in G2V mode or V2G modes, respectively.

Assuming that there are  $n$  number of modules, grid AC current of individual modules can be denoted by  $i_n$ . If efficiency of the  $n^{th}$  module in V2G and G2V modes are expressed as  $\eta_{V2G,n}$  and  $\eta_{G2V,n}$ , respectively, then  $n$  number of functions can be written for each operating mode. In each mode, efficiency can be written in terms of grid current as follows:

$$\eta_{G2V,n} = f_{G2V,n}(i_n) \quad (2)$$

$$\eta_{V2G,n} = f_{V2G,n}(i_n) \quad (3)$$

Overall efficiency function will define a surface in an  $(n+1)$ -dimensional space. In a system with  $n$  number of modules, overall efficiency in G2V mode can be expressed as follows:

$$\eta_{G2V} = \frac{f_{G2V,1}(i_1) \cdot i_1 + f_{G2V,2}(i_2) \cdot i_2 + \dots + f_{G2V,n}(i_n) \cdot i_n}{i_1 + i_2 + \dots + i_n} \quad (4)$$

Also, overall efficiency of a system in V2G mode with  $n$  number of modules can be expressed as:

$$\eta_{V2G} = \frac{i_1 + i_2 + \dots + i_n}{\frac{i_1}{f_{V2G,1}(i_1)} + \frac{i_2}{f_{V2G,2}(i_2)} + \dots + \frac{i_n}{f_{V2G,n}(i_n)}} \quad (5)$$

The purpose of the optimization algorithm is to maximize  $\eta_{G2V}$  and  $\eta_{V2G}$  using the available information. This maximization can be expressed as a constrained optimization problem with three constraints. First, the sum of individual AC grid charging currents in G2V mode and in V2G mode should be equal to the total demand from the utility grid in either mode. Second, grid currents of individual modules should be positive in G2V mode and negative in V2G mode. Note that, all the modules will only be operating at the same designated mode simultaneously, i.e. V2G or G2V. Last, steady-state

grid current cannot exceed the rated current of the individual modules.

The cost function of this optimization problem is the overall efficiency function of the system for either mode. The optimization problem should be formulated so as to minimize the cost function, thus reciprocal of  $\eta_{G2V}$  and  $\eta_{V2G}$  should be used when formulating the problem. Since  $\eta_{G2V}$  and  $\eta_{V2G}$  are always positive and cannot be zero, using the reciprocal will not pose an issue mathematically. The optimization problem can be expressed for both V2G and G2V operation modes. In G2V mode;

$$\min \frac{\sum_{k=1}^n i_k}{\sum_{k=1}^n f_{G2V,k}(i_k) \cdot i_k} \quad (6)$$

subject to

$$\sum_{k=1}^n i_k = i_{demand} \quad (7)$$

$$[i_1 \quad i_2 \quad \dots \quad i_n] \leq i_{rated} \quad (8)$$

$$[-i_1 \quad -i_2 \quad \dots \quad -i_n] < 0 \quad (9)$$

In V2G mode;

$$\min \frac{\sum_{k=1}^n \frac{i_k}{f_{V2G,k}(i_k)}}{\sum_{k=1}^n i_k} \quad (10)$$

subject to

$$\sum_{k=1}^n i_k = i_{demand} \quad (11)$$

$$[-i_1 \quad -i_2 \quad \dots \quad -i_n] \leq i_{rated} \quad (12)$$

$$[i_1 \quad i_2 \quad \dots \quad i_n] < 0 \quad (13)$$

Numerous methods can be used to solve the above optimization problem. When the number of modules are less than a certain number, brute force method can be utilized. However, when the number of modules is increased, the dimension of the optimization problem will also increase and it will be much more difficult to use the brute force. Then, a heuristic algorithm, such as particle swarm optimization (PSO) or artificial bee colony (ABC) algorithm can be utilized to solve the  $n$ -dimensional optimization problem.

### III. SIMULATION RESULTS

Simulations for the system are carried out in two different mediums. Conceptual simulation with the ideal circuit elements is carried out in PLECS to get fast results for the general operation of a single module and the whole system. Considerably more detailed simulations with the actual models provided from the manufacturers are carried out in LTspice to get more accurate and detailed results in correspondence with the real world operation of the system.

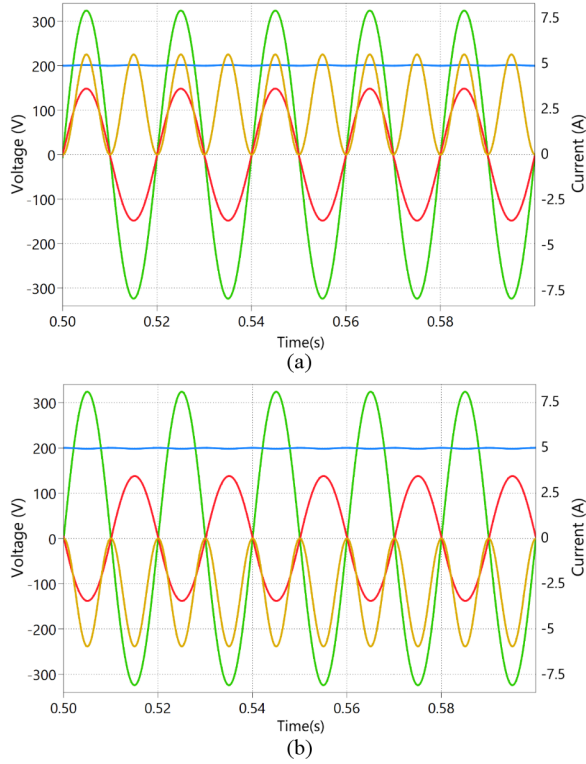


Fig. 3. Simulation results of a single module. (a) Grid to vehicle charging,  $\delta = 0.25$ . (b) Vehicle to grid discharging,  $\delta = -0.25$ . (green: grid voltage, red: grid current, blue: battery voltage, yellow: battery current)

#### A. Single Module Operation

As the first step in system design, the operation of a single module is verified. Modulation scheme described in [22] is implemented using the C-block in PLECS. When everything except  $\delta$  in (1) is held constant,  $\delta$  can be used to control amount of current and/or power to be delivered. Moreover, when its sign is changed, current also changes direction, leading to bidirectional power flow. This modulation scheme has three major benefits; open loop power factor correction, easy controllability of power, and soft switching of semiconductor switches.

Simulation setup is built considering 220 V rms AC grid voltage, 200 V battery bank voltage and a rated power of 600 W. Battery bank is modeled using a constant DC voltage source. Semiconductor and passive circuit elements only have resistive parasitics and all other parameters are assumed to be ideal. Simulation results obtained from PLECS show very low current harmonics and unity power factor as shown in Fig. 3. It is also verified that, grid AC charging current command can be tracked accurately for different operating points. However, the grid current waveform in PLECS is obtained using an averaging block. In real world application, an LC filter will be utilized to filter out switching ripple from the input current. This will introduce a certain amount of reactive power to the charger, causing a slight phase shift between voltage and current.

#### B. Modular Operation

Modular operation is verified in PLECS using two individual modules in single-phase. Phase-shift ratio defined in (1) is

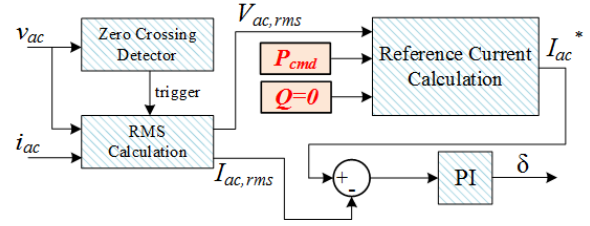


Fig. 4. Controller block diagram.

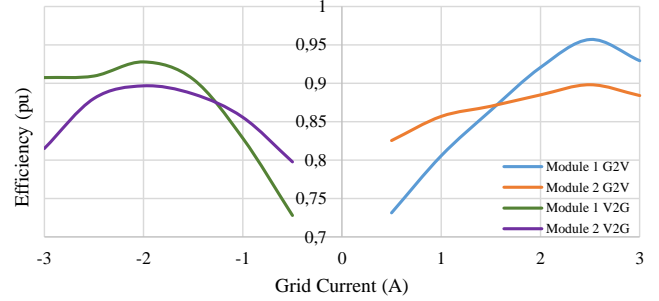


Fig. 5. Hypothetical efficiency curves for simulation.

used to control the amount of power or current to be delivered. An AC current reference generated by the master controller based on the desired operating point of the individual chargers is fed to the controller of the charger modules. Block diagram is depicted in Fig. 4.

Modular system simulation should verify the benefits of the developed optimization controller by comparing the efficiency increase between equal current sharing and optimized current sharing. The proposed modular system should have higher overall efficiency at light to moderate loads compared to a modular system in which all the modules are operated at balanced power. Since there is no working hardware prototype during the simulations yet, two modules with hypothetical load-efficiency curves are assumed as shown in Fig. 5. Normally, the efficiency curves of two identical modules should not be much different from each other; however in the proposed modular system two different modules based on the same topology but having a different characteristics can also be used. In this study, we also aim to minimize the impacts of the differences of the modules in the overall operation of the system.

The system is first tested in equal current sharing mode in which the modules are loaded equally for all demand values. In other words, utility grid command is divided equally among all modules considering their operating limits. Therefore, for this testing, no efficiency increase technique is used, and the modules operate as if there is only one charger module. Then, it is tested in optimized current sharing mode. For this testing, it is assumed that utility grid demand can change over time, and thereby, the master controller runs the proposed optimization algorithm and determines the new AC grid charge current values for each individual modules. In order to verify the operation of the optimization algorithm, these two cases are simulated in PLECS and the resulting efficiency curves are compared as depicted in Fig. 6. When the modules are

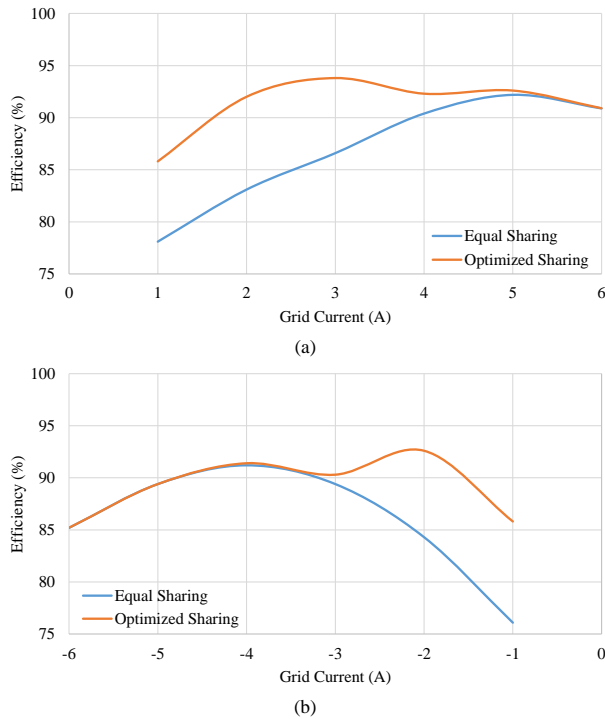


Fig. 6. Efficiency comparison of equal sharing and optimized sharing. (a) G2V mode. (b) V2G mode.

operated in equal current sharing mode, the resulting efficiency curve of the system is not much different from the ones of individual modules where it presents low efficiency from light to moderate loads. On the other hand, optimized current sharing operation improves efficiency by up to 8.9% in G2V mode and up to 9.7% in V2G mode. When heavy penetration of EVs into the utility grid is considered in the future, this efficiency increase can translate into big amounts of energy savings over time.

#### IV. EXPERIMENTAL RESULTS

Experimental setup is built for one module for single-phase 220 V rms grid AC voltage, 180 V DC battery bank voltage at a rated power of 600 W. Due to availability of only one-module, the proposed optimization algorithm is implemented with this module (i.e. second module is assumed to operate in parallel with this module). The lab experiments are conducted at lower voltage and power levels than stated above for safety reasons, i.e.  $V_i=120$  V,  $V_{bat}=120$  V. From (1), by fixing voltage levels as stated before and by choosing,  $n=50/17$ ,  $L=16\mu\text{H}$ ,  $f_s=25$  kHz and  $f_i=50$  Hz,  $\delta$  can be varied between  $\pm 0.3$  to control power up to 400 W. Fig. 7(a) shows the experimental setup and Fig. 7(b) shows the individual charger module. Also, the components used in the development of the hardware prototype are listed in Table I.

The experimental results show very low current harmonics, almost unity power factor and bidirectional power flow as can be seen in Fig. 8. The efficiency is 91.4% in case (a) and 90.1% in case (b). As shown in Fig. 8, the experimental results are in-line with simulation results of a single module. The easy controllability of the charger is tested and verified for bidirectional power flow. Therefore, the results show

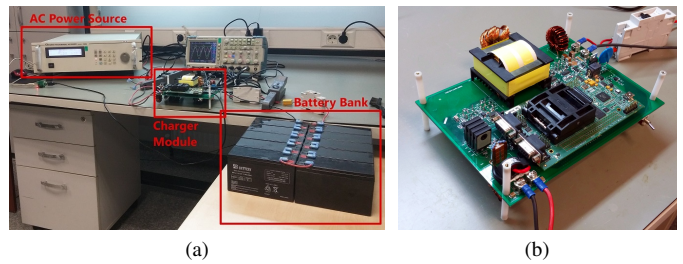


Fig. 7. (a) Experimental setup. (b) Charger module.

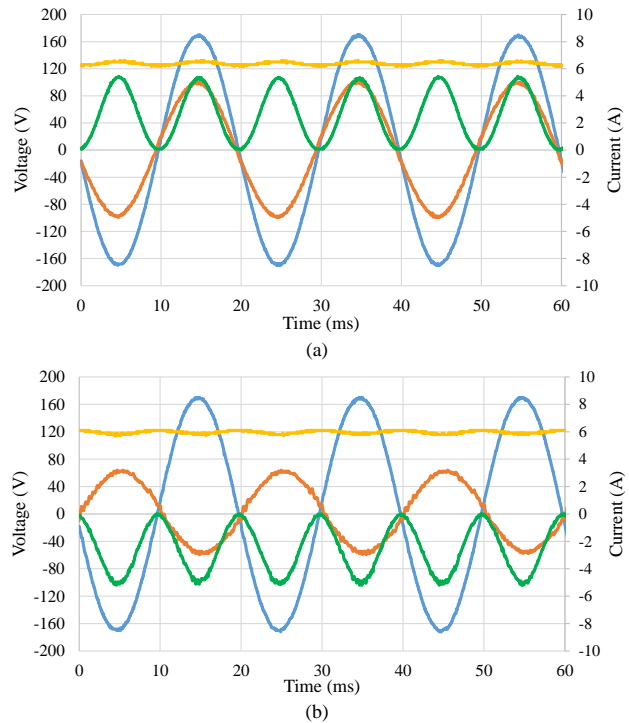


Fig. 8. Experimental results of a single module. (a). Grid to vehicle charging. (b) Vehicle to grid discharging. (blue: grid voltage, red: grid current, yellow: battery voltage, green: battery current.)

that as more modules are added in parallel, the developed optimization algorithm can be implemented to increase overall efficiency without any problem.

#### V. CONCLUSIONS

A modular charger design is proposed for improving efficiency for a wide load range for a bidirectional EV charger unit through optimized current sharing method. The idea is verified in simulations, and a hardware prototype is built for bench-top testing. Initial data gathered from the first prototype show promising results regarding the verification of the proposed operation of the individual modules for increased efficiency operation. For future work, current sharing optimization algorithm and efficiency improvement will be verified with the two charger modules.

#### ACKNOWLEDGMENT

The authors would like to thank ELSIS AS., Ankara, Turkey for their support in providing circuit elements and testing equipment for the design.

TABLE I  
COMPONENT LIST FOR THE HARDWARE PROTOTYPE

Part	Manufacturer	Part Number	Details
Sync. Rect MOSFETs	Infineon	IPW60R045CP	650V, 60A
AC and DC side MOSFETs	IXYS	IXFH32N50Q	500V, 32A
Transformer	EPCOS	B66395GX197	Primary: 6x0.5 mm enameled copper wire, 50 turns Secondary: 30x0.5mm enameled copper wire, 17 turns
Power Inductor	Magnetics Inc.	55550	16 $\mu$ H, 20x0.5mm enameled copper wire, 16 turns
AC Filter Inductor	Magnetics Inc.	77930A7	320 $\mu$ H, 1.2 mm enameled copper wire, 48 turns
DC Filter Inductor	Magnetics Inc.	77930A7	80 $\mu$ H, 1.2 mm enameled copper wire, 24 turns
AC/DC Filter Capacitors	TDK	CGA9P3X7T2E225M250KE	16x2.2 $\mu$ F caps. for AC side, 20x2.2 $\mu$ F caps. for DC side
Battery Bank	SB. Battery	SP7.2-12	10 units of 12V/7.2 Ah lead-acid batteries in series
Microcontroller	Texas Ins.	TMS320F28335	

## REFERENCES

- [1] J. Hu, S. You, M. Lind, and J. Ostergaard, "Coordinated charging of electric vehicles for congestion prevention in the distribution grid," *IEEE Trans. Smart Grid*, vol. 5, no. 2, pp. 703–711, March 2014.
- [2] M. J. E. Alam, K. M. Muttaqi, and D. Sutanto, "A controllable local peak-shaving strategy for effective utilization of PEV battery capacity for distribution network support," *IEEE Trans. Ind. Appl.*, vol. 51, no. 3, pp. 2030–2037, 2015.
- [3] L. Igualada, C. Corchero, M. Cruz-Zambrano, F. Heredia *et al.*, "Optimal energy management for a residential microgrid including a vehicle-to-grid system," *IEEE Trans. Smart Grid*, vol. 5, no. 4, pp. 2163–2172, 2014.
- [4] G. Del-Rosario-Calaf, M. Cruz-Zambrano, C. Corchero, and R. Gumara-Ferret, "Distribution network congestion management by means of electric vehicle smart charging within a multi-microgrid environment," in *IEEE Int. Elect. Vehicle Conf. (IEVC)*, Dec 2014, pp. 1–8.
- [5] T. S. Ustun, U. Cali, and M. C. Kisacikoglu, "Energizing microgrids with plug-in electric vehicles and distributed generators during emergencies," in *IEEE Int. Telecommun. Energy Conf. (INTELEC)*, Oct 2015, pp. 1–6.
- [6] M. C. Kisacikoglu, B. Ozpineci, and L. M. Tolbert, "EV/PHEV bidirectional charger assessment for V2G reactive power operation," *IEEE Trans. Power Electron.*, vol. 28, no. 12, pp. 5717–5727, Dec 2013.
- [7] M. C. Kisacikoglu, M. Kesler, and L. M. Tolbert, "Single-phase on-board bidirectional PEV charger for V2G reactive power operation," *IEEE Trans. Smart Grid*, vol. 6, no. 2, pp. 767–775, 2015.
- [8] G. E. Sfakianakis, J. Everts, and E. A. Lomonova, "Overview of the requirements and implementations of bidirectional isolated AC-DC converters for automotive battery charging applications," in *10<sup>th</sup> Int. Conf. Ecological Vehicles and Renewable Energies (EVER)*, March 2015, pp. 1–12.
- [9] S. S. Williamson, A. K. Rathore, and F. Musavi, "Industrial electronics for electric transportation: Current state-of-the-art and future challenges," *IEEE Trans. Ind. Electron.*, vol. 62, no. 5, pp. 3021–3032, May 2015.
- [10] A. Khaligh and S. Dusmez, "Comprehensive topological analysis of conductive and inductive charging solutions for plug-in electric vehicles," *IEEE Trans. Veh. Technol.*, vol. 61, no. 8, pp. 3475–3489, Oct 2012.
- [11] M. Yilmaz and P. T. Krein, "Review of battery charger topologies, charging power levels, and infrastructure for plug-in electric and hybrid vehicles," *IEEE Trans. Power Electron.*, vol. 28, no. 5, pp. 2151–2169, May 2013.
- [12] F. Musavi, M. Edington, W. Eberle, and W. G. Dunford, "Evaluation and efficiency comparison of front end AC-DC plug-in hybrid charger topologies," *IEEE Trans. Smart Grid*, vol. 3, no. 1, pp. 413–421, March 2012.
- [13] Y. S. Kim, W. Y. Sung, and B. K. Lee, "Comparative performance analysis of high density and efficiency PFC topologies," *IEEE Trans. Power Electron.*, vol. 29, no. 6, pp. 2666–2679, June 2014.
- [14] H. Wang, S. Dusmez, and A. Khaligh, "Design and analysis of a full-bridge LLC-based PEV charger optimized for wide battery voltage range," *IEEE Trans. Veh. Technol.*, vol. 63, no. 4, pp. 1603–1613, May 2014.
- [15] F. Musavi, W. Eberle, and W. G. Dunford, "A high-performance single-phase bridgeless interleaved PFC converter for plug-in hybrid electric vehicle battery chargers," *IEEE Trans. Ind. Appl.*, vol. 47, no. 4, pp. 1833–1843, July 2011.
- [16] B. Whitaker, A. Barkley, Z. Cole, B. Passmore, D. Martin, T. R. McNutt, A. B. Lostetter, J. S. Lee, and K. Shiozaki, "A high-density, high-efficiency, isolated on-board vehicle battery charger utilizing silicon carbide power devices," *IEEE Trans. Power Electron.*, vol. 29, no. 5, pp. 2606–2617, May 2014.
- [17] D. S. Gautam, F. Musavi, M. Edington, W. Eberle, and W. G. Dunford, "An automotive onboard 3.3-kw battery charger for PHEV application," *IEEE Trans. Veh. Technol.*, vol. 61, no. 8, pp. 3466–3474, Oct 2012.
- [18] J. Deng, S. Li, S. Hu, C. C. Mi, and R. Ma, "Design methodology of LLC resonant converters for electric vehicle battery chargers," *IEEE Trans. Veh. Technol.*, vol. 63, no. 4, pp. 1581–1592, May 2014.
- [19] J. Y. Lee and H. J. Chae, "6.6-kW onboard charger design using DCM PFC converter with harmonic modulation technique and two-stage DC/DC converter," *IEEE Trans. Ind. Electron.*, vol. 61, no. 3, pp. 1243–1252, March 2014.
- [20] S. Li, J. Deng, and C. C. Mi, "Single-stage resonant battery charger with inherent power factor correction for electric vehicles," *IEEE Trans. Veh. Technol.*, vol. 62, no. 9, pp. 4336–4344, Nov 2013.
- [21] C. Y. Oh, D. H. Kim, D. G. Woo, W. Y. Sung, Y. S. Kim, and B. K. Lee, "A high-efficient nonisolated single-stage on-board battery charger for electric vehicles," *IEEE Trans. Power Electron.*, vol. 28, no. 12, pp. 5746–5757, Dec 2013.
- [22] N. D. Weise, G. Castellino, K. Basu, and N. Mohan, "A single-stage dual-active-bridge-based soft switched AC-DC converter with open-loop power factor correction and other advanced features," *IEEE Trans. Power Electron.*, vol. 29, no. 8, pp. 4007–4016, Aug 2014.
- [23] J. Everts, F. Krismer, J. V. den Keybus, J. Driesen, and J. W. Kolar, "Optimal ZVS modulation of single-phase single-stage bidirectional DAB AC-DC converters," *IEEE Trans. Power Electron.*, vol. 29, no. 8, pp. 3954–3970, Aug 2014.
- [24] T. Thandapani and R. Arumugam, "Modular power supply for telecom application (54v/100a)," in *IEEE Int. Symp. Ind. Electron.*, vol. 2, July 2006, pp. 1334–1340.
- [25] C. Wang, M. Xu, F. C. Lee, and Z. Luo, "Light load efficiency improvement for multi-channel PFC," in *IEEE Power Electron. Specialists Conf.*, June 2008, pp. 4080–4085.
- [26] L. Zhang, K. Sun, Y. Xing, L. Feng, and H. Ge, "A modular grid-connected photovoltaic generation system based on DC bus," *IEEE Trans. Power Electron.*, vol. 26, no. 2, pp. 523–531, Feb 2011.
- [27] J. Mei, B. Xiao, K. Shen, L. M. Tolbert, and J. Y. Zheng, "Modular multilevel inverter with new modulation method and its application to photovoltaic grid-connected generator," *IEEE Trans. Power Electron.*, vol. 28, no. 11, pp. 5063–5073, Nov 2013.
- [28] B. Xiao, L. Hang, J. Mei, C. Riley, L. M. Tolbert, and B. Ozpineci, "Modular cascaded h-bridge multilevel PV inverter with distributed MPPT for grid-connected applications," *IEEE Trans. Ind. Appl.*, vol. 51, no. 2, pp. 1722–1731, March 2015.
- [29] B. Savage, R. Shuttleworth, and N. Schofield, "A modular battery charger for electric vehicles," in *IEEE Energy Conversion Congr. Expo. (ECCE)*, Sept 2013, pp. 3600–3606.
- [30] M. Vasiladiotis, A. Rufer, and A. Bguin, "Modular converter architecture for medium voltage ultra fast EV charging stations: Global system considerations," in *IEEE Int. Elect. Vehicle Conf.*, March 2012, pp. 1–7.
- [31] L. R. Chen, S. L. Wu, D. T. Shieh, and T. R. Chen, "Sinusoidal-ripple-current charging strategy and optimal charging frequency study for li-ion batteries," *IEEE Trans. Ind. Electron.*, vol. 60, no. 1, pp. 88–97, Jan 2013.
- [32] Y. D. Lee and S. Y. Park, "Electrochemical state-based sinusoidal ripple current charging control," *IEEE Trans. Power Electron.*, vol. 30, no. 8, pp. 4232–4243, Aug 2015.